# Estimation of Transmission Dynamics of COVID-19 in India: The Influential Saturated Incidence Rate

- Tanvi
*University of Delhi*

Rajiv Aggarwal
*University of Delhi*

Ashutosh Rajput
*University of Delhi*

### Recommended Citation

# Estimation of Transmission Dynamics of COVID-19 in India: The Influential Saturated Incidence Rate

[1]**Tanvi,** [2,*]**Rajiv Aggarwal and** [3]**Ashutosh Rajput**

[1]Department of Mathematics
Shaheed Rajguru College of
Applied Sciences for Women
University of Delhi
New Delhi-110096, India
tanvihrc@gmail.com

[2]Department of Mathematics
Deshbandhu College
University of Delhi
New Delhi-110019, India
rajiv_agg1973@yahoo.com

[3]Department of Mathematics
Faculty of Mathematical
Sciences
University of Delhi
New Delhi-110007, India
ashuhrc14@gmail.com

*Corresponding Author

## Abstract

A non-linear SEIR mathematical model for coronavirus disease in India has been proposed, by incorporating the saturated incidence rate on the occurrence of new infections. In the model, the threshold quantity known as the reproduction number is evaluated which determines the stability of disease-free equilibrium and the endemic equilibrium points. The disease-free equilibrium point becomes globally asymptotically stable when the corresponding reproduction number is less than unity, whereas, if it is greater than unity then the endemic equilibrium point comes into existence, which is locally asymptotically stable under certain restrictions on the parameters value in the model. The impact of various parameters on the threshold quantity is signified by the sensitivity analysis. Numerical results imply that by implementing and strictly following the prevention measures a rapid reduction in the reproduction number for COVID-19 can be observed, through which the coronavirus disease can be controlled.

1046

Applications and Applied Mathematics: An International Journal (AAM), Vol. 15 [2020], Iss. 2, Art. 21

AAM: Intern. J., Vol. 15, Issue 2 (December 2020)                                    1047

# 1.   Introduction

Coronavirus disease (COVID-19) is a transmissible disease caused by a newly discovered coronavirus. COVID-19 is a new epidemic and the hazardous coronavirus turned-up in Wuhan, China, in the month of December 2019. Before that outbreak of COVID-19 disease in China, the world was not well known to it. According to the World Health Organization (2020a), there are three ways of transmission of COVID-19 virus defined as:

(1)  Symptomatic transmission: The transmission of virus from an infected individual who is experiencing the symptoms of coronavirus and can infect others.

(2)  Pre-symptomatic transmission: The transmission of virus by people who don't look or feel sick, but will eventually get symptoms later. They can also infect others even without getting symptoms (CNN report (2020)).

(3)  Asymptomatic transmission: The transmission of the virus by infected people who do not have symptoms and will never get symptoms from their infection, but these infected carriers could still infect others (CNN report (2020)).

By globally affecting many countries, COVID-19 has now become a pandemic. By the end of September 25, 2020, a report from WHO says that worldwide confirmed cases of COVID-19 were $32,755,202$ (Worldometer (2020a)) and total deceased had reached $992,979$ with the case fatality rate about $3.03\%$. Recent worldwide data indicate that the cluster of cases is a major reason for increasing the incidence of COVID-19 on a large scale.

In India, community transmission was initially a reason for the spread of COVID-19. As reported by the World Health Organization (2020b), the cluster of cases has now become a major concern for it. As of September 25, 2020, total confirmed cases of COVID-19 in India were around $5,901,571$ also, total deceased has crossed $93,410$. In India, the number of infected people recovered from the COVID-19 disease is more than $4,900,000$. According to the World Health Organization (2020c), individuals infected with other immune based comorbidities are more vulnerable to become infected with coronavirus, which has majorly led to more than $70\%$ deaths due to COVID-19 disease in India. The government of India, has advised not to travel the highly infected regions and quarantine to those who are returning from such regions. As this pandemic has become a severe concern in India, the government has restricted international travelling to stop disease transmission (Colbourn (2020); World Health Organization (2020a)).

Mathematical modeling is an important instrument to understand the real-world problems. So far, many efforts have been taken into account to develop realistic mathematical models together with the investigation of the transmission dynamics of infectious diseases and the researchers are still working to improve it. The disease can be supervised by forecasting the importance of public health interventions and predicted patterns of epidemics, which in turn help to formulate the epidemiological model.

Many researchers started to work with the basic SIR and SEIR models to understand the transmission dynamics of infectious diseases (Awoke and Semu (2018); Pradhan et al. (2019); Tanvi and Aggarwal (2020b); Tanvi et al. (2020); Yaghoubi and Najafi (2020); Wang et al. (2009)). Manyombe et al. (2020) proposed a mathematical model to describe the viral infection of HIV-1 with both cell-to-cell and virus-to cell transmission together with four distributed delays. Nowadays, many researchers have also started considering more realistic mathematical models with saturated incidence rate than the bilinear incidence rate ($\beta IS$), in order to capture the behavioural changes of population when infected population increases (Liu (2019); Liu and Yang (2012)). Hsu and Hsieh (2005) have proposed a mathematical model by incorporating the saturated incidence rate induced by quarantine and other prevention measures implemented by the health authorities in addition to the behavior changes observed in the population to avoid infection. Dongmei and Ruan (2007) described an SIR model by considering nonmonotonic incidence rate to describe the psychological effects of certain infectious diseases on the society. The global outbreak of COVID-19 attracts the curiosity of researchers to work upon it. Several mathematical modeling problems have been proposed by the researchers to interpret the transmission of COVID-19 (Annas et al. (2020); Ahmad et al. (2020); Chen et al. (2020); Kucharski et al. (2020); Mandal et al. (2020); Pang et al. (2020); Prem et al. (2020); Quaranta et al. (2020); Shahidul et al. (2020); Wilder-Smith and Freedman (2020); Zhang et al. (2020)). In an article of Yang and Wang (2020), they suggested a mathematical model comprising both environment to human and human to human routes for the transmission of coronavirus. The transmissibility rate of super spreaders in a mathematical model for the spread of COVID-19 disease is discussed by Ndairou et al. (2020) and they investigated the sensitivity analysis of the model corresponding to different parameters. Lin et al. (2020), studied the government actions and behavioural reaction of individuals as control measures to propose a conceptual model.

In accordance with the above mentioned papers, we have introduced a non-linear mathematical model by introducing the saturated incidence rate to anticipate the effect of prevention measures that create obstructions in the transmission of COVID-19 disease from infectives to susceptibles. Therefore, we have introduced a Holling type-II (Dubey et al. (2013)) function as the incidence rate. The Holling type-II function signifies the fact that when the number of infected individuals is very large then the improvement through behavioural changes (infection prevention, self quarantine and isolation) can be observed in susceptibles as well as infectives in order to create hindrance in the spread of infection and this may happen because of media or self awareness amongst individuals. At this time, upholding the role of government strategies is a prerequisite; that is, a continuance of quarantine, social distancing, isolation of infectives and adequate treatment facility to minimize the COVID-19 disease from the population. All the quantitative and qualitative analysis of the proposed model have been done using Perko (1991) and Strogatz (2014).

The paper is organized in the following manner. A non-linear mathematical model to study the transmission dynamics of COVID-19 has been proposed in the second section. Together with, the location and existence of the disease-free and the endemic equilibrium points, we have estimated the reproduction number in the third section. The fourth section deals with the stability analysis of the disease free equilibrium and the endemic equilibrium points. In the fifth section, the sensitivity analysis of the reproduction number with respect to various parameters is determined. In the sixth

Applications and Applied Mathematics: An International Journal (AAM), Vol. 15 [2020], Iss. 2, Art. 21

AAM: Intern. J., Vol. 15, Issue 2 (December 2020)                    1049

section, the system is solved numerically to signify the impact of prevention measures on disease spread. In the seventh section, we concluded the results with a brief discussion.
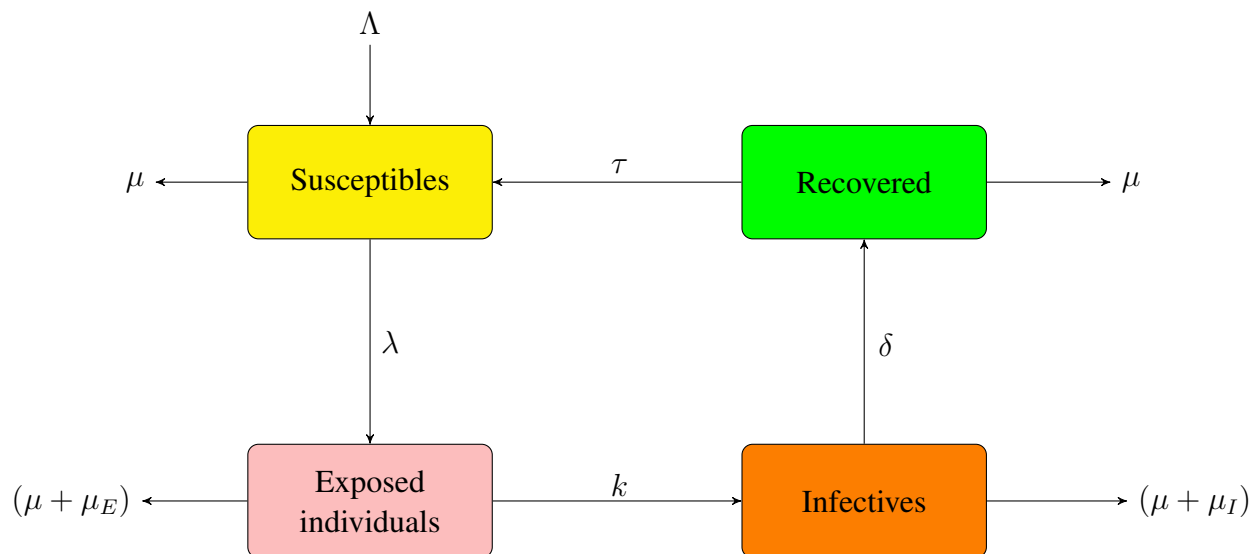
## 2.    Model formation

In this section, we have introduced a non-linear SEIR mathematical model by incorporating a saturated incidence rate, to describe the transmission dynamics of COVID-19. To begin with the model, we assume that the population is homogeneously distributed. A constant recruitment rate $\Lambda$ is presumed, with which population is entering into the class of susceptibles. Further we do not distinguish between asymptomatic infected individuals and symptomatic infectives as both of them are contagious and as reported by (ECDC (2020)), there is no significant difference in their viral load. For formulating the model, the total population $N(t)$ is divided into four mutually exclusive compartments defined as

- $S(t)$ - the class of population susceptible to COVID-19 disease.

- $E(t)$ - the class of pre-symptomatic individuals exposed to coronavirus, capable to infect other.

- $I(t)$ - the class of symptomatic and asymptomatic infected individuals.

- $R(t)$ - the class of population recovered from the disease.

Thus, the total population $N(t)$ is given as

$$N(t) = S(t) + E(t) + I(t) + R(t).$$



**Figure 1.** Schematic diagram of mutually distinct classes for the COVID-19 model

Susceptibles receive infection of COVID-19 disease, after having an effective contact with exposed or infected individuals. The force of infection, $\lambda$, associated with the transmission is a Holling type-II function given as

$$\lambda = \beta \left( \frac{\eta E}{1 + \gamma_1 E} + \frac{I}{1 + \gamma_2 I} \right). \tag{1}$$

In the expression of $\lambda$, a parameter $\beta$ denotes the transmission rate of infection. The modification parameter $\eta < 1$, signifies that the exposed individuals have less viral load than the infected individuals to spread the infection. Terms $\frac{1}{1+\gamma_1 E}$ and $\frac{1}{1+\gamma_2 I}$ (contributing a vital role in the model) measure the inhibition effect from the behavioural change of exposed individuals and infectives, corresponding to increment in the number of exposed and infected individuals, respectively. The term $\gamma_1$, determines the behavioural changes such as infection prevention and social distancing taken under consideration by uninfected population. Infection prevention comprises various measures such as rigorous hand-washing schemes, respiratory etiquettes and the use of surgical face masks. The term social distancing focuses on reducing physical contact between infectives and susceptibles as a means of interrupting transmission of coronavirus. There are various kinds of social distancing measures such as individual level social distancing which includes quarantine of individuals, having close contact with a newly detected infected individual and measures affecting groups of individuals, which consists the restriction of mass gatherings, closure of workplaces, educational institutes, border closures and travelling restrictions. Whereas, the term $\gamma_2$ measures the effectiveness of facilities provided by the healthcare authorities, which comprises isolation of infectives, establishing treatment facilities for sub-intensive and intensive care needs together with reducing the workload on healthcare workers. The effectiveness of these interventions increases with increase in the number of exposed and infected populations, which in result decrease the number of new infections. It can be observed in the following expression:

$$\lim_{E,I \to \infty} \beta \left( \frac{\eta E}{1 + \gamma_1 E} + \frac{I}{1 + \gamma_2 I} \right) = \beta \left( \frac{\eta}{\gamma_1} + \frac{1}{\gamma_2} \right).$$

Thus, the saturated incidence rate is more effective as it prevents the unboundedness of the force of infection considering suitable parameters.

At the rate $\lambda S$, susceptibles switch into the exposed class. It is assumed that, after remaining under the incubation period, exposed individuals proceed to the class of infectives, with the progression rate $kE$, where $k$ is a progression coefficient (indicates the inverse of incubation period). After taking treatment of the disease, the number of infectives headway to the class of recovered individuals by the rate $\delta I$, as $\delta$ is the recovery rate of infectives. Further, evidence from other coronavirus infections (SARS and MERS) suggest that recovered individuals are likely to be immune from re-infection as a result of development of antibodies in their body as reported by ECDC (2020). However, it is assumed that a small fraction of these individuals will not get permanent immunity due to compromised immune systems and hence become susceptible again at the rate $\tau$. The model is described along with a schematic diagram given in Figure (1). By considering the above described facts and definition of various parameters, the mathematical representation of the model

Applications and Applied Mathematics: An International Journal (AAM), Vol. 15 [2020], Iss. 2, Art. 21

AAM: Intern. J., Vol. 15, Issue 2 (December 2020) 1051

**Table 1.** Description of parameters for the COVID-19 model

| Parameter | Description |
|:---:|:---|
| $\Lambda$ | constant recruitment rate |
| $\beta$ | transmission rate for coronavirus |
| $\mu$ | natural death rate |
| $\mu_E$ | disease induced death rate of exposed individuals |
| $\mu_I$ | disease induced death rate of infectives |
| $k$ | progression rate from exposed class to infected class |
| $\delta$ | recovery rate of infected individuals |
| $\tau$ | progression rate from recovered to susceptible class |
| $\gamma_1$ | effectiveness of behavior change in exposed individuals |
| $\gamma_2$ | effectiveness of behavior change in infected individuals |
| $\eta$ | modification parameter |

is

$$
\begin{aligned}
\frac{dS}{dt} &= \Lambda - \lambda S + \tau R - \mu S, \\
\frac{dE}{dt} &= \lambda S - kE - (\mu + \mu_E)E, \\
\frac{dI}{dt} &= kE - \delta I - (\mu + \mu_I)I, \\
\frac{dR}{dt} &= \delta I - \tau R - \mu R,
\end{aligned}
\tag{2}
$$

with the initial conditions given as

$$
S(0) = S_0 \geqslant 0, \ E(0) = E_0 \geqslant 0, \ I(0) = I_0 \geqslant 0 \text{ and } R(0) = R_0 \geqslant 0.
\tag{3}
$$

### 2.1. Basic properties of the model

To prove that the model is well posed, all the solution components $S(t), \ E(t), \ I(t)$ and $R(t)$ must be positive for all time $t \geqslant 0$, as all the classes imply human population. This can be easily verified by following Tanvi and Aggarwal (2020a). Based on biological reasons, the following feasible region will be considered

$$
\Omega = \left\{ (S, E, I, R) \in \mathbb{R}_+^4 : N(t) \leqslant \frac{\Lambda}{\mu} \right\}.
$$

Now, to prove the boundedness of the components of solution, we observe that

$$
N'(t) = \Lambda - \mu N(t) - \mu_E E - \mu_I I \leqslant \Lambda - \mu N(t).
$$

Thus, we obtain

$$
\frac{dN}{dt} + \mu N \leqslant \Lambda,
$$

from which we get

$$N(t) \leqslant N(0)e^{-\mu t} + \frac{\Lambda}{\mu}(1 - e^{-\mu t}).$$

Therefore, if $N(0) \leqslant \frac{\Lambda}{\mu}$, we get $0 < N(t) \leqslant \frac{\Lambda}{\mu}$. This proves the boundedness of $N(t)$ and in turn, $N(t)$ proves the boundedness of all the components of solution for the model. Thus, mathematically the model system (2) is a well-posed model. Based on the above discussion, we state the following theorem.

**Theorem 2.1.**

For the model system (2), together with the initial conditions given by (3), all the solution components $S(t)$, $E(t)$, $I(t)$ and $R(t)$ are positive for $t \geqslant 0$. Further, the region $\Omega$ is positively invariant; that is, all the solutions starting in $\Omega$ remain in $\Omega$.

## 3.    Equilibrium points

In this section, we determine the basic reproduction number and the equilibrium points to describe the steady state of the model system (2). The equilibrium points for the model system (2) can be determined by solving the following system of simultaneous equations:

$$\begin{aligned}
\Lambda - \lambda S + \tau R - \mu S &= 0, \\
\lambda S - kE - (\mu + \mu_E)E &= 0, \\
kE - \delta I - (\mu + \mu_I)I &= 0, \\
\delta I - \tau R - \mu R &= 0.
\end{aligned} \tag{4}$$

A state when no coronavirus infection is present in the population is described by the disease-free equilibrium point for the model system (2), computed as

$$Q_0 = \left( \frac{\Lambda}{\mu}, 0, 0, 0 \right). \tag{5}$$

### 3.1.    The basic reproduction number

The basic reproduction number, denoted by $\mathcal{R}_0$, is a threshold quantity which calculates the average number of secondary infections generated by a single infected individual in an entirely susceptible population (Jones (2007)). It measures the contagiousness of the disease and informs about the urgency of implementing the prevention measures to avoid the disastrous situation. It majorly depends on three factors:

- The probability of acquiring infection when an infected individual comes in contact with a susceptible.
- The average rate of contact between susceptibles and infectives.

Applications and Applied Mathematics: An International Journal (AAM), Vol. 15 [2020], Iss. 2, Art. 21

AAM: Intern. J., Vol. 15, Issue 2 (December 2020) 1053

- The duration of infectiousness of infectives.

To evaluate the basic reproduction number by using the next-generation matrix approach (Driessche and Watmough (2002)), we compute matrices $V$ and $F$ corresponding to the transfer and the new infection terms, respectively. Matrices $V$ and $F$ are given as

$$F = \begin{bmatrix} \eta\beta\frac{\Lambda}{\mu} & \beta\frac{\Lambda}{\mu} \\ 0 & 0 \end{bmatrix} \quad \text{and} \quad V = \begin{bmatrix} k + \mu + \mu_E & 0 \\ -k_1 & \delta + \mu + \mu_I \end{bmatrix}.$$

Therefore, by calculating $FV^{-1}$ we obtain the basic reproduction number $\mathcal{R}_0 = \rho(FV^{-1})$, as

$$\mathcal{R}_0 = \beta\eta\frac{\Lambda}{\mu(k + \mu + \mu_E)} + \beta k\frac{\Lambda}{\mu(k + \mu + \mu_E)(\delta + \mu + \mu_I)}. \tag{6}$$

### 3.2. The endemic equilibrium point

After solving the system of equations given by (4) in terms of the force of infection $\lambda$, the endemic equilibrium point for the model system (2) is obtained as $Q^* = (S^*, E^*, I^*, R^*)$. The components of $Q^*$ are given as follows

$$
\begin{aligned}
S^* &= \frac{\Lambda(k + \mu + \mu_E)(\delta + \mu + \mu)(\tau + \mu)}{(k + \mu + \mu_E)(\delta + \mu + \mu)(\tau + \mu)(\lambda + \mu) - \delta k\lambda\tau}, \\
E^* &= \frac{\Lambda\lambda(\delta + \mu + \mu)(\tau + \mu)}{(k + \mu + \mu_E)(\delta + \mu + \mu)(\tau + \mu)(\lambda + \mu) - \delta k\lambda\tau}, \\
I^* &= \frac{\Lambda k\lambda(\tau + \mu)}{(k + \mu + \mu_E)(\delta + \mu + \mu)(\tau + \mu)(\lambda + \mu) - \delta k\lambda\tau}, \\
R^* &= \frac{\Lambda\delta k\lambda}{(k + \mu + \mu_E)(\delta + \mu + \mu)(\tau + \mu)(\lambda + \mu) - \delta k\lambda\tau}.
\end{aligned}
\tag{7}
$$

We can compute the force of infection $\lambda$, by using the expression

$$\lambda = \beta\left(\frac{\eta E^*}{1 + \gamma_1 E^*} + \frac{I^*}{1 + \gamma_2 I^*}\right).$$

After some algebraic calculations, we obtain that $\lambda$ satisfies the following cubic equation

$$A_2\lambda^3 + A_1\lambda^2 + A_0\lambda = 0, \tag{8}$$

where

$$
\begin{aligned}
A_2 &= (\delta k\tau)^2 + \gamma_1\gamma_2 k\Lambda^2 VW^2 + \gamma_2 k\Lambda UVW^2 + \gamma_1\Lambda UV^2W^2 + (UVW)^2 \\
&\quad - \delta k\Lambda\tau W(\gamma_2 k + \gamma_1 V) - 2\delta k\tau UVW, \\
A_1 &= \Lambda kUVW^2(\gamma_2\mu - \beta) + \Lambda UV^2W^2(\gamma_1\mu - \beta\eta) + 2\mu(UVW)^2 + \delta k^2\Lambda\tau\beta W \\
&\quad + \delta k\Lambda\eta\beta\tau VW - 2\delta k\tau\mu UVW - (\gamma_1 + \eta\gamma_2)k\Lambda^2\beta VW^2, \\
A_0 &= (\mu UVW)^2 - \beta\Lambda\mu UVW^2(\eta V + k).
\end{aligned}
\tag{9}
$$

In the expression given by (9), the terms, $U, V$ and $W$ are computed as

$$U = k + \mu + \mu_E,$$
$$V = \delta + \mu + \mu_I,$$
$$W = \tau + \mu.$$

From Equation (8), we get

$$\text{either } \lambda = 0 \text{ or } A_2\lambda^2 + A_1\lambda + A_0 = 0. \tag{10}$$

The term $\lambda = 0$, gives the disease-free equilibrium point and $\lambda^*$ satisfying the quadratic equation in (10), corresponds to the unique endemic equilibrium point. The endemic equilibrium point exists, if all the components of $Q^*$ are positive, which is possible, only if the force of infection ($\lambda$) is positive.

It can be easily observed that $A_2 > 0$, whereas, $A_0 < 0$ only if $\mathcal{R}_0 > 1$. Thus, by Descarte's rule of sign, the quadratic equation $A_2\lambda^2 + A_1\lambda + A_0 = 0$ has a unique positive real root $\lambda$ when $\mathcal{R}_0 > 1$, which proves the existence and uniqueness of the endemic equilibrium point $Q^* = (S^*, E^*, I^*, R^*)$ for $\mathcal{R}_0 > 1$. We summarize the above discussion in the following theorem.

**Theorem 3.1.**

The unique endemic equilibrium point $Q^* = (S^*, E^*, I^*, R^*)$ for the model system (2) exists, if $\mathcal{R}_0 > 1$.

## 4.    Stability analysis of the equilibrium points

In this segment, the stability analysis has been performed to visualize the behavior of solution trajectories near the equilibrium points.

**Theorem 4.1.**

The disease-free equilibrium point $Q_0$, for the model system (2) is locally asymptotically stable, if $\mathcal{R}_0 < 1$ and is unstable, otherwise.

***Proof:***

The Jacobian matrix corresponding to the model system (2) is evaluated at the disease-free equilibrium point $Q_0$, given as

$$J_0 = \begin{bmatrix} -\mu & -\eta\beta\frac{\Lambda}{\mu} & -\beta\frac{\Lambda}{\mu} & \tau \\ 0 & \eta\beta\frac{\Lambda}{\mu} - (k+\mu+\mu_E) & \beta\frac{\Lambda}{\mu} & 0 \\ 0 & k & -(\delta+\mu+\mu_I) & 0 \\ 0 & 0 & \delta & -(\mu+\tau) \end{bmatrix}.$$

The characteristic equation of $J_0$ is

$$(\lambda + \mu)(\lambda + (\mu + \tau))(\lambda^2 + C_1\lambda + C_0) = 0,$$

where

$$C_1 = (k + \mu + \mu_E) + (\delta + \mu + \mu_I) - \eta\beta\frac{\Lambda}{\mu},$$

$$C_0 = (k + \mu + \mu_E)(\delta + \mu + \mu_I) - \beta\frac{\Lambda}{\mu}\left(\eta(\delta + \mu + \mu_I) + k\right).$$

The first two linear factors give two eigenvalues, as $\lambda_1 = -\mu$ and $\lambda_2 = -(\mu + \tau)$. The remaining quadratic factor is $\lambda^2 + C_1\lambda + C_0 = 0$. In a quadratic factor, $C_0$ and $C_1$ are positive only if $R_0 < 1$. Therefore, according to the Routh-Hurwitz criterion both the roots of $\lambda^2 + C_1\lambda + C_0 = 0$ have negative real parts, if $\mathcal{R}_0 < 1$. Thus, for $\mathcal{R}_0 < 1$, all the eigenvalues of $J_0$ have a negative real part. Therefore, the disease-free equilibrium point is locally asymptotically stable, if the corresponding reproduction number is less than unity and is unstable, otherwise. ∎

For proving the global stability of the disease-free equilibrium point by following Castillo-Chavez et al. (1999), we rewrite the model system (2) as

$$\frac{dU}{dt} = F(U, I),$$
$$\frac{dI}{dt} = G(U, I), \qquad (11)$$
$$G(U, 0) = 0,$$

where $U$ denotes the number of uninfected individuals and $I$ denotes the number of infected individuals. According to Castillo-Chavez et al. (1999), the following two conditions are sufficient to guarantee the global stability of the disease-free equilibrium point $(U_0, 0)$:

(H1)  For $\frac{dU}{dt} = F(U, 0)$, $U_0$ is globally asymptotically stable,

(H2)  $G(U, I) = AI - \hat{G}(U, I)$, where $\hat{G}(U, I) \geqslant 0$ for $(U, I) \in G'$,

where $A = D_I G(U_0, 0)$ is a M-matrix and $G'$ is a region, where the model makes biological sense.

**Theorem 4.2.**

The disease-free equilibrium point $Q_0 = (\frac{\Lambda}{\mu}, 0, 0, 0)$ for the model system (2), is globally asymptotically stable, if $\mathcal{R}_0 < 1$ and the conditions expressed in $(H1)$ and $(H2)$ are satisfied.

*Proof:*

In the previous theorem the local asymptotic stability of $Q_0$ has been proved for $\mathcal{R}_0 < 1$. Thus, the global stability of $Q_0$ can only be proved in the region where $\mathcal{R}_0 < 1$. For this, we let $U = (S, R)^T \in \mathbb{R}_+^2$ be the vector whose coordinates represent the uninfected classes of population and $I = (E, I)^T \in \mathbb{R}_+^2$ be the vector whose coordinates represent the two infected classes of population. Here, $Q_0 = (U_0, 0)$, where $U_0 = (\frac{\Lambda}{\mu}, 0)$. For the model system (2), $F(U, I)$ of equation

(11) can be written as

$$F(U, I) = \begin{bmatrix} \Lambda - \lambda S + \tau R - \mu S \\ \delta I - \tau R - \mu R \end{bmatrix}.$$

Hence,

$$F(U, 0) = \begin{bmatrix} \Lambda + \tau R - \mu S \\ -(\tau + \mu)R \end{bmatrix}.$$

It is obvious that, $U_0 = \left(\frac{\Lambda}{\mu}, 0\right)$ is globally asymptotically stable for $F(U, 0)$.

Now, for condition $(H2)$ we consider

$$G(U, I) = \begin{bmatrix} \lambda S - (k + \mu + \mu_E)E \\ kE - (\delta + \mu + \mu_I)I_T \end{bmatrix}.$$

We also have, $G(U, I) = AI - \hat{G}(U, I),$ from which we obtain

$$\hat{G}(U, I) = \begin{bmatrix} \hat{G}_1(U, I) \\ \hat{G}_2(U, I) \end{bmatrix} = \begin{bmatrix} \beta\frac{\Lambda}{\mu}(\eta E + I) - \beta S\left(\eta\frac{E}{1+\gamma_1 E} + \frac{I}{1+\gamma_2 I}\right) \\ 0 \end{bmatrix}$$

$$\geqslant \begin{bmatrix} \beta\frac{\Lambda}{\mu}\left(\eta E \frac{\gamma_1 E}{1+\gamma_1 E} + I\frac{\gamma_2 I}{1+\gamma_2 I}\right) \\ 0 \end{bmatrix}.$$

It can be clearly seen that $\hat{G}(U, I) \geqslant 0$. Thus, both the conditions $(H1)$ and $(H2)$ are satisfied, which prove the global asymptotic stability of the disease-free equilibrium point for $\mathcal{R}_0 < 1$. Epidemiologically, it means the disease can be eradicated from the population in the long run, if the corresponding reproduction number is less than unity.                                                ∎

Now, for the model system (2), we define four new variables $S = x_1$, $E = x_2$, $I = x_3$, and $R = x_4$, to illustrate the local asymptotic stability of the endemic equilibrium point $Q^*$, in such a manner that $x_1 + x_2 + x_3 + x_4 = 1$. Thus, the model system (2), can be expressed as

$$\begin{aligned} \frac{dx_1}{dt} &= \Lambda - \lambda x_1 + \tau x_4 - \mu x_1, \\ \frac{dx_2}{dt} &= \lambda x_1 - (k + \mu + \mu_E)x_2, \\ \frac{dx_3}{dt} &= kx_2 - (\delta + \mu + \mu_I)x_3, \\ \frac{dx_4}{dt} &= \delta x_3 - (\mu + \tau)x_4. \end{aligned} \tag{12}$$

The force of infection $\lambda$, can be expressed as

$$\lambda = \frac{\eta\beta x_2}{1 + \gamma_1 x_2} + \frac{\beta x_3}{1 + \gamma_2 x_3}.$$

Applications and Applied Mathematics: An International Journal (AAM), Vol. 15 [2020], Iss. 2, Art. 21

AAM: Intern. J., Vol. 15, Issue 2 (December 2020) 1057

The linearization matrix for the model system (2) evaluated at the disease-free equilibrium point $Q_0$, is obtained as

$$
J_0 = \begin{bmatrix}
-\mu & -\eta\beta\frac{\Lambda}{\mu} & -\beta\frac{\Lambda}{\mu} & \tau \\
0 & \eta\beta\frac{\Lambda}{\mu} - (k + \mu + \mu_E) & \beta\frac{\Lambda}{\mu} & 0 \\
0 & k & -(\delta + \mu + \mu_I) & 0 \\
0 & 0 & \delta & -(\mu + \tau)
\end{bmatrix}.
$$

After letting $\mathcal{R}_0 = 1$, we obtain the bifurcation parameter as:

$$
\beta = \beta^* = \frac{\mu}{\Lambda}\left[\frac{(\delta + \mu + \mu_I)(k + \mu + \mu_E)}{\eta(\delta + \mu + \mu_I) + k}\right].
$$

It is straightforward to observe that $0$ is a simple eigenvalue, corresponding to the matrix $J_0$ for $\mathcal{R}_0 = 1$. Also for $\mathcal{R}_0 = 1$, it can be observed in theorem (4.1) that $C_1$ is positive. Thus, the remaining three eigenvalues of $J_0$ have negative real parts. Therefore, we can decompose the neighbourhood of the disease-free equilibrium point into a one dimensional center manifold and a three-dimensional stable manifold. Thus, the center manifold theory (Carr (1981)) can be used to investigate the local stability of the endemic equilibrium point $Q^*$. For convenience, the theorem given by Castillo-Chavez and Song (2004) to determine the local stability of the endemic equilibrium point is stated as follows.

**Theorem 4.3.**

Consider, the following general system of ordinary differential equations with a parameter $\phi$:

$$
\frac{dx}{dt} = f(x, \phi), \tag{13}
$$
$$
f : \mathbb{R}^n \times \mathbb{R} \to \mathbb{R} \text{ and } C^2(\mathbb{R}^n \times \mathbb{R}),
$$

where $0$ is an equilibrium point of the system (that is, $f(0, \phi) = 0$ for all $\phi$), and assume

(1) $A = D_x f(0,0) = \left(\frac{df_i}{dx_j}(0,0)\right)$ is the linearization matrix of system (13) at the equilibrium $0$ and $\phi$ evaluated at $0$. Zero is a simple eigenvalue of $A$ and all other eigenvalues of $A$ have a negative real part.

(2) Matrix $A$ has a right eigenvector $w$ and a left eigenvector $v$ (each corresponding to the zero eigenvalue).

Let $f_k$ be the $k_{th}$ component of $f$ and

$$
a = \sum_{k,j,i=1}^{n} v_k w_i w_j \frac{\partial^2 f_k}{\partial x_i \partial x_j}(0,0), \quad b = \sum_{k,i=1}^{n} v_k w_i \frac{\partial^2 f_k}{\partial x_i \partial \phi}(0,0). \tag{14}
$$

The local dynamics of the system around $0$ is totally determined by the signs of $a$ and $b$.

(a) $a > 0, b > 0$. When $\phi < 0$ with $|\phi| << 1, 0$ is locally asymptotically stable and there exists a positive unstable equilibrium; when $0 < \phi << 1$, $0$ is unstable and there exists a negative, locally asymptotically stable equilibrium point.

(b) $a < 0, b < 0$. When $\phi < 0$ with $|\phi| << 1, 0$ is unstable; when $0 < \phi << 1$, $0$ is locally asymptotically stable and there exists a positive, unstable equilibrium point.

(c) $a > 0, b < 0$. When $\phi < 0$ with $|\phi| << 1$, $0$ is unstable and there exists a negative, locally asymptotically stable equilibrium; when $0 < \phi << 1$, $0$ is stable and a positive unstable equilibrium appears.

(d) $a < 0, b > 0$. When $\phi$ changes sign from negative to positive, $0$ changes its stability from stable to unstable. Correspondingly, a negative unstable equilibrium becomes positive and locally asymptotically stable.

Now, we have to compute the right and left eigenvectors corresponding to the matrix $J_0$. The right eigenvector of the matrix $J_0$ is $w = [w_1, w_2, w_3, w_4]$, with its components computed as

$$w_1 = \frac{\beta^* \Lambda (k + \mu + \mu_E)}{\mu(\eta \beta^* - \mu(k + \mu + \mu_E))}, \quad w_2 = \frac{\beta^* \Lambda}{\mu(k + \mu + \mu_E)}, \quad w_3 = 1 \text{ and } w_4 = \frac{\delta}{\tau + \mu}.$$

The components of the left eigenvector $v = [v_1, v_2, v_3, v_4,]$ satisfying $v J_0 = 0$, are obtained as

$$v_1 = 0, \quad v_2 = 1, \quad v_3 = \frac{\beta^* \Lambda}{\mu(\delta + \mu + \mu_I)} \text{ and } v_4 = 0.$$

**Computation of a and b.** Now, by computing the partial derivatives of $f_2$ and $f_3$ with respect to $x_1, x_2, x_3, x_4$ and $\beta^*$, the non-zero partial derivatives evaluated at the disease-free equilibrium point are obtained as

$$\frac{\partial^2 f_2}{\partial x_1 \partial x_2} = \eta \beta^*, \quad \frac{\partial^2 f_2}{\partial x_1 \partial x_3} = \beta^*, \quad \frac{\partial^2 f_2}{\partial x_2^2} = -2\eta \beta^* \frac{\Lambda \gamma_1}{\mu}, \quad \frac{\partial^2 f_2}{\partial x_3^2} = -2\beta^* \frac{\Lambda \gamma_2}{\mu},$$

$$\frac{\partial^2 f_2}{\partial x_2 \partial \beta^*} = \eta \frac{\Lambda}{\mu} \text{ and } \frac{\partial^2 f_2}{\partial x_3 \partial \beta^*} = \frac{\Lambda}{\mu}.$$

Thus, the values for $a$ and $b$ are computed as

$$a = \sum_{k,j,i=1}^{4} v_k w_i w_j \frac{\partial^2 f_k}{\partial x_i \partial x_j}(0,0),$$

$$= 2\beta^* \frac{\Lambda}{\mu} \left( \frac{\tau \mu(k + \mu + \mu_E)}{(\mu + \tau)(\mu(k + \mu + \mu_I) - \eta \beta^*)} - \gamma_2 - \frac{\beta^* \mu^2(k + \mu + \mu_I)^2 + \eta \beta^* \gamma_1 \Lambda^2}{(\mu(k + \mu + \mu_I) - \eta \beta^* \Lambda)^2} \right),$$

$$b = \sum_{k,i=1}^{4} v_k w_i \frac{\partial^2 f_k}{\partial x_i \partial \beta^*}(0,0),$$

$$= v_2 \left( w_2 \frac{\partial^2 f_2}{\partial x_2 \partial \beta^*} + w_3 \frac{\partial^2 f_2}{\partial x_3 \partial \beta^*} \right),$$

$$= \frac{\Lambda}{\mu}(\eta w_2 + w_3) > 0.$$

It can be observed that $a < 0$, only if

$$\gamma_2 > \frac{\tau \mu(k + \mu + \mu_E)}{(\mu + \tau)(\mu(k + \mu + \mu_I) - \eta \beta^*)} - \frac{\beta^* \mu^2(k + \mu + \mu_I)^2 + \eta \beta^* \gamma_1 \Lambda^2}{(\mu(k + \mu + \mu_I) - \eta \beta^* \Lambda)^2}. \tag{15}$$

Therefore, the interior endemic equilibrium point for the model system (2), is locally asymptotically stable for $\mathcal{R}_0 > 1$ and $\beta^* < \beta$, with $\beta$ close to $\beta^*$, if Equation (15) holds. The above discussion can be summarized in the following theorem.

Applications and Applied Mathematics: An International Journal (AAM), Vol. 15 [2020], Iss. 2, Art. 21

AAM: Intern. J., Vol. 15, Issue 2 (December 2020) 1059

**Theorem 4.4.**

The endemic equilibrium point $Q^*$ corresponding to the model system (2) is locally asymptotically stable for $\mathcal{R}_0 > 1$, if

$$\gamma_2 > \frac{\tau\mu(k+\mu+\mu_E)}{(\mu+\tau)(\mu(k+\mu+\mu_I)-\eta\beta^*)} - \frac{\beta^*\mu^2(k+\mu+\mu_I)^2+\eta\beta^*\gamma_1\Lambda^2}{(\mu(k+\mu+\mu_I)-\eta\beta^*\Lambda)^2}. \tag{16}$$

Further, if Equation (16) holds, the system exhibits a supercritical transcritical bifurcation at $\mathcal{R}_0 = 1$, with $\beta = \beta^*$ as a bifurcation parameter.

## 5. Sensitivity analysis

In this segment, the significance of sensitivity of the threshold quantity, $\mathcal{R}_0$, to the parameters of the model is discussed. Sensitivity analysis is commonly used to acknowledge the vitality of model prediction to parameters value. Due to the common occurrence of errors, while using presumed parameters value and collecting data, determination of the relative importance of the various factors becomes imperative, that may affect transmission and prevalence of the disease. Therefore, it is important to study the relative change in the reproduction number with respect to a parameter. In respect of this, the ratio of the relative change in a variable to the relative change in a parameter provides the normalized forward sensitivity index. The normalized forward sensitivity index, assists to determine how to reduce human morbidity and mortality due to a disease. Alternatively, the sensitivity index can be evaluated on the basis of partial derivatives, provided that a variable can be differentiated with respect to a parameter.

**Definition 5.1.**

The normalized forward sensitivity index of a variable, $u$, that depends differentiably on a parameter $p$, is defined as Chitnis et al. (2008)

$$\Upsilon_p^u := \frac{\partial u}{\partial p}\frac{p}{u}. \tag{17}$$

With respect to all existing parameters in the threshold quantity, $\mathcal{R}_0$, the sensitivity of $\mathcal{R}_0$ determines the parameters having an immense impact on the reproduction number, $\mathcal{R}_0$. By using parameters value given in Table 3, the sensitivity indices will be given.

By using the sensitivity index of $\mathcal{R}_0$ to the parameters, we have analyzed the following points:

- From $\Upsilon_\beta^{\mathcal{R}_0} = 1$, we deduce that with the increment (reduction) of any fraction of amount in the transmission rate $\beta$, $\mathcal{R}_0$ also increases (decreases) by the same fraction. Therefore, as transmission rate gets lower, the disease also vanishes from the community.
- From $\Upsilon_\Lambda^{\mathcal{R}_0} = 1$, we can conclude that, with the gain (fall) of $10\%$ in the recruitment rate $\Lambda$, $\mathcal{R}_0$ also increases(decreases) by 10%, which may lead to an epidemic.
- From $\Upsilon_\delta^{\mathcal{R}_0} = -0.541474$, it can be observed that increasing the recovery rate $\delta$ for infectives by $10\%$, the reproduction number diminishes by $5.41474\%$. Therefore, the faster recovery of infected individuals will give the rapid reduction in the reproduction number.

**Table 2.** Sensitivity indices of $\mathcal{R}_0$ to the parameters value

| parameter | Sensitivity index $(\mathcal{R}_0)$ |
|:---:|:---:|
| $\beta$ | 1 |
| $\Lambda$ | 1 |
| $k$ | $-0.358669$ |
| $\mu$ | $-1.00069$ |
| $\mu_E$ | $-0.00199523$ |
| $\mu_I$ | $-0.0971727$ |
| $\delta$ | $-0.541474$ |
| $\eta$ | $0.361054$ |

- From $\Upsilon_\eta^{\mathcal{R}_0} = 0.361054$, it can be realized that $\mathcal{R}_0$ changes positively by $3.61054\%$ as $\eta$ increases by $10\%$. That is, as $\eta$ reduces, exposed individuals transmit COVID-19 disease with a lower rate, which in turn helps to reduce the reproduction number, $\mathcal{R}_0$.

From the above observations, it can be figured out that the sensitivity indices provide vital information by analyzing the mathematical model with the data taken into account.

## 6.    Numerical simulations

In this section, we perform numerical simulations to analyze the model and justify the analytical results. The disease COVID-19 had already affected India at the beginning of the month of March 2020. By the end of September 2020 in India, COVID-19 has become a pandemic disease. We simulate the non-linear model by estimating the data which include the number of confirmed cases, active cases, recovered cases and deaths due to coronavirus during the month of September 2020 (that is, from September 1, 2020 to September 25, 2020), to study the transmission dynamics of COVID-19 in India. Therefore, the initial number of susceptibles is chosen as $S(0) = 1.3 \times 10^9$ (MoHFW (2020)), with initial conditions for the remaining classes as $E(0) = 1,022,200$, $I(0) = 800,127$ and $R(0) = 2,836,945$. Now, we will discuss the estimation of parameters value.

The estimated value of baseline parameters are computed from COVID-19 data sources such as the Worldometer (2020b), World Health Organization (2020a) and the published literature. In India, the daily number of births ranges between $45,000 - 70,000$ (India population live (2020)), therefore, we have assumed the constant recruitment rate $\Lambda$ to be $50,000$. The transmission rate for COVID-19 disease is fitted according to the transmission pattern of coronavirus in India at $\beta = 6.4 \times 10^{-11}$. The parameter $\mu$, denoting the natural death rate, is estimated to be $\frac{1}{69.3} \times \frac{1}{365} = 3.9 \times 10^{-5}$ per day, where 69.3 years is the average life expectancy of an individual in India (Statista (2020)). For the time interval September 01, 2020 to September 25, 2020, the average number of deaths per day was estimated at $1,119$ and the average number of new cases at $88,545$ that are evaluated using the daily number of deaths and daily new cases, respectively (Worldometer (2020b)). Thus, the disease induced death rate of infectives $(\mu_I)$ is estimated as
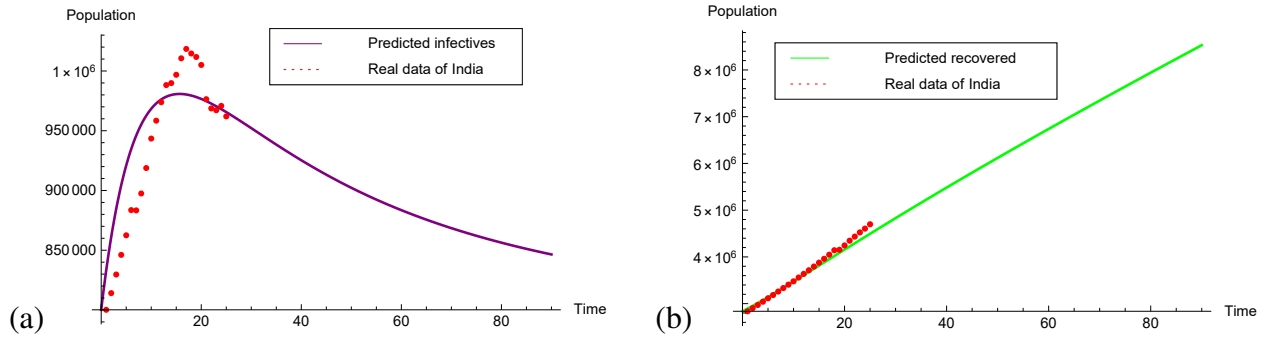
Applications and Applied Mathematics: An International Journal (AAM), Vol. 15 [2020], Iss. 2, Art. 21

AAM: Intern. J., Vol. 15, Issue 2 (December 2020)                                                  1061

**Table 3.** Set of parameters value for COVID-19 in India

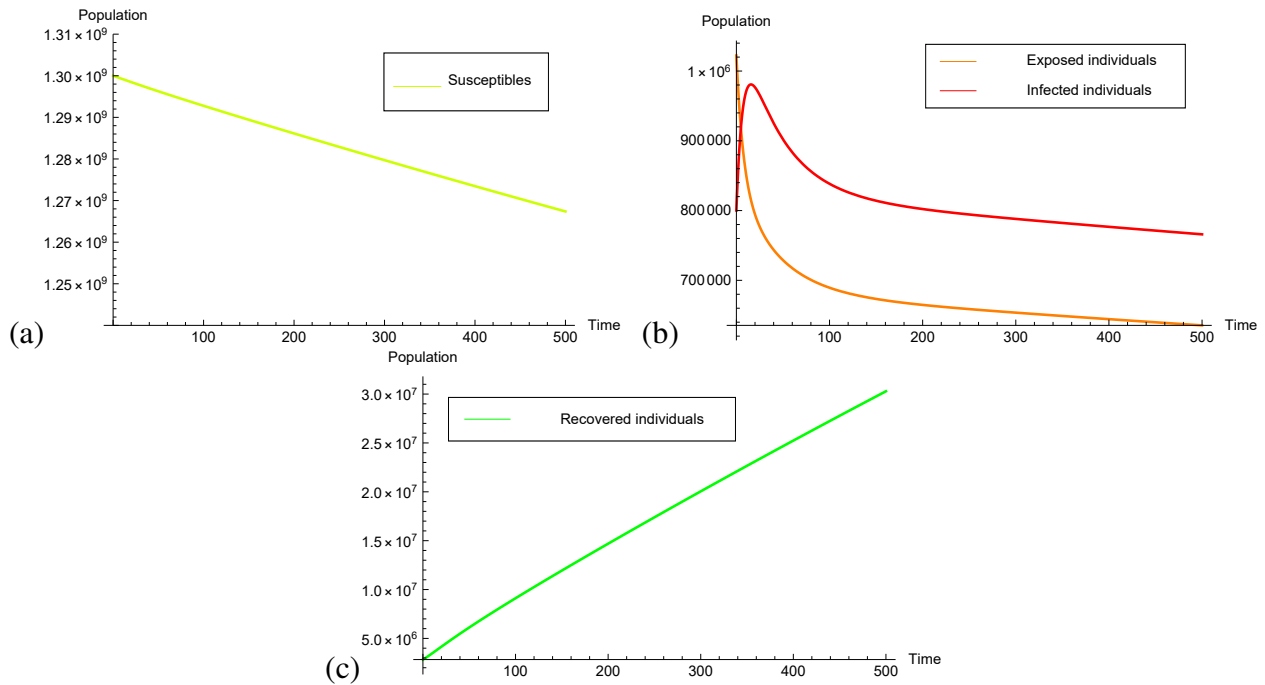| Parameter | Value | Source |
|---|---|---|
| $\Lambda$ | 50000 day $^{-1}$ | Estimated, (India population live (2020)) |
| $\beta$ | $6.4 \times 10^{-11}$ day $^{-1}$ | Fitted |
| $\mu$ | 0.000039 day $^{-1}$ | Estimated, (Statista (2020)) |
| $\mu_E$ | 0.0002 day $^{-1}$ | Assumed |
| $\mu_I$ | 0.012638 day $^{-1}$ | Estimated, (Worldometer (2020b)) |
| $k$ | 1/10 day $^{-1}$ | Estimated, (MoHFW (2020)) |
| $\delta$ | 1/14 day $^{-1}$ | Estimated |
| $\tau$ | 0.0001 day $^{-1}$ | Fitted |
| $\gamma_1$ | $8.5 \times 10^{-7}$ | Assumed |
| $\gamma_2$ | $6.8 \times 10^{-7}$ | Assumed |
| $\eta$ | 0.68 | Fitted |

the per day case fatality rate due to COVID-19, at $\mu_I = 0.012638$ day$^{-1}$. As exposed individuals have only mild infection and may have compromised immune systems due to other immune based comorbidities, therefore, we have assumed the number of deaths of exposed individuals as $\mu_E = 0.0002$ day$^{-1}$. According to MoHFW (2020), the average incubation period for COVID-19 ranges between $1 - 12.5$ days, that is, a time between exposure to the virus and onset of symptoms. Therefore, we have data fitted the progression rate from exposed class to infected class at $k = \frac{1}{10}$ day$^{-1}$.

According to Ferguson et al. (2013), the average time an infective spent in hospital is $8$ days. Further, after getting treatment in the hospital, an individual needs to be under isolation for the next $6$ days. Thus, on an average the number of days an infective needs to recover completely is $14$ days, from which we have estimated the recovery rate per day at $\delta = \frac{1}{14}$ day$^{-1}$. It is observed that the recovered individuals from COVID-19 infection get immuned for a few months. However, an individual with compromised immune system may not gain sufficient immunity, and hence, becomes susceptible again. Thus, the value of $\tau$ is assumed at $0.0001$ (fitted according to the data of India). In the model, $\gamma_1$ and $\gamma_2$ are the prevention measures taken by exposed and infected individuals, respectively. A small increment in $\gamma_1$ and $\gamma_2$ diminish the force of infection significantly, therefore, we have assumed $\gamma_1 = 8.5 \times 10^{-7}$ and $\gamma_2 = 6.8 \times 10^{-7}$. The modification parameter $\eta = 0.68$ (in force of infection) indicates that exposed individuals have less viral load to spread the COVID-19 disease infection in relation to the infected individuals.

To validate the proposed model and estimated parameters value, the time series plot of real data from September 1, 2020 to September 25, 2020 with the predicted solution trajectory of the model system for the time interval September 1 - November 30, 2020 , has been shown in Figure 2. From Figure 2(a) and 2(b), it can be observed that by the end of November 30, 2020, the predicted number of actively infected cases of COVID-19 will reach around $850,000$ whereas, the number of recovered cases will be approximately $9,000,000$. Thus, to accommodate a large number of infectives in quarantine centres and hospitals, the health care authorities are required to be equipped with sufficient treatment facilities.
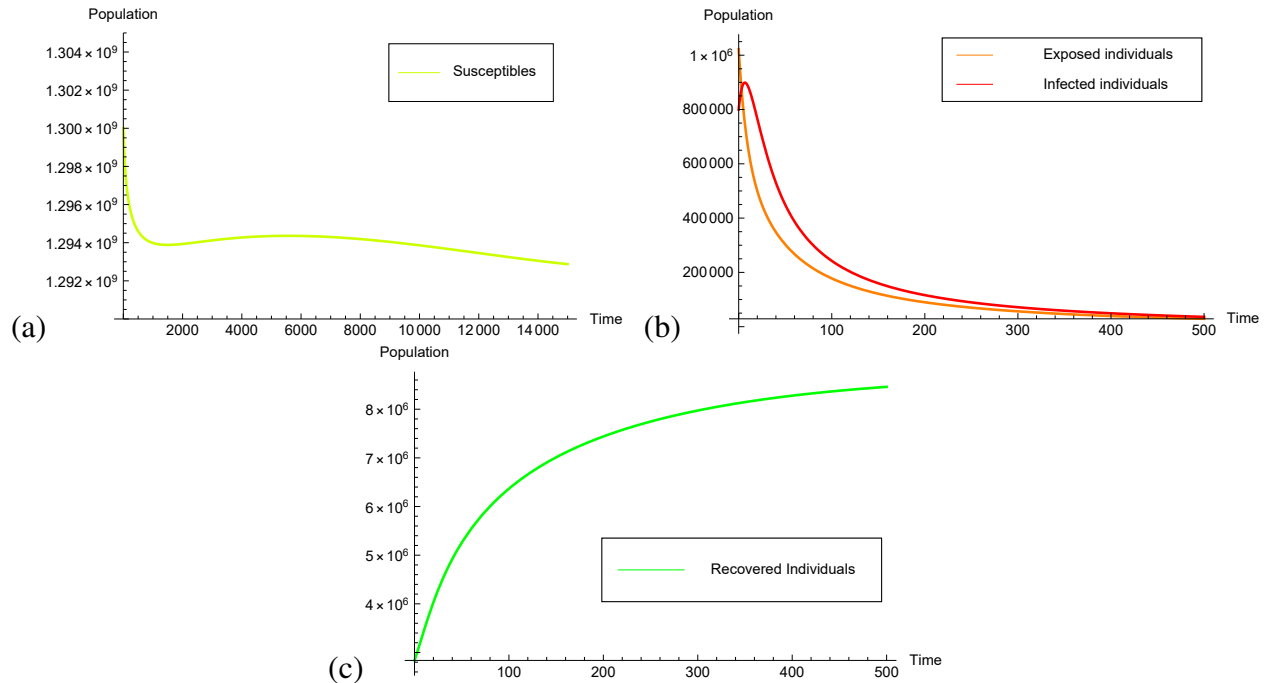
**Figure 2.** Time series plot showing the least square fit of the model system to real data of India (a) Population infected from COVID-19 (b) Population recovered from COVID-19. The red dots represent the real data of India for infectives and recovered individuals and the solid lines represent the prediction given by the model for COVID-19



**Figure 3.** Graphs indicating the prevalence of COVID-19 infection when the reproduction number for the COVID-19 is greater than unity
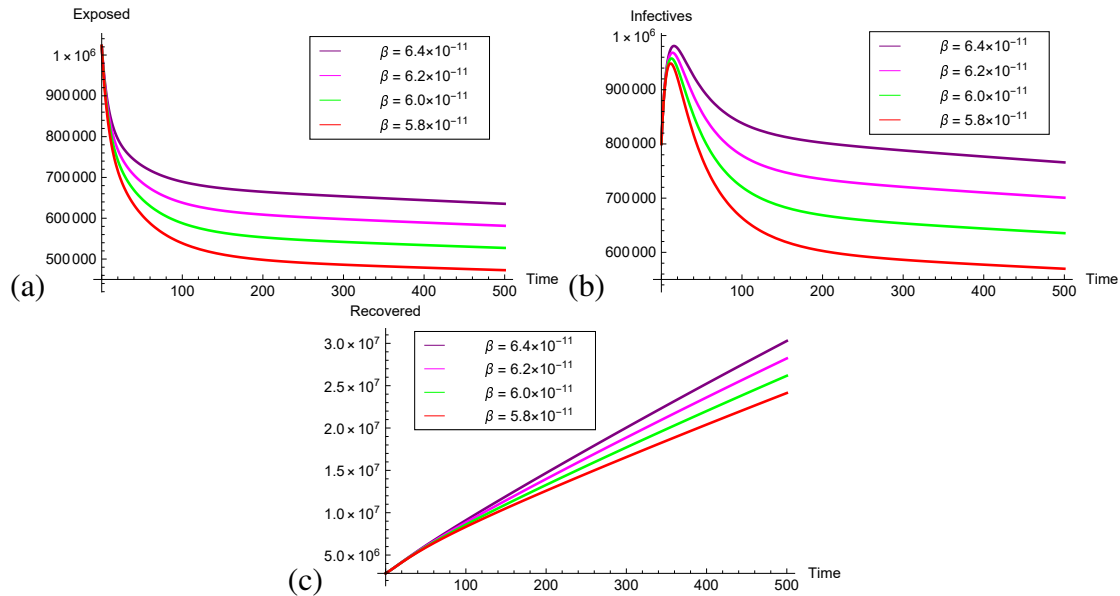
In Figure 3, the graphs illustrated the results obtained for $\mathcal{R}_0 > 1$ by exercising the parameters value as given in Table (3). Due to disobeying the rules implemented by the government (not effectively following social distancing and isolation rules), the transmission rate of COVID-19 in India has reached to $\beta = 6.4 \times 10^{-11}$. Thus, the reproduction number is estimated at $\mathcal{R}_0 = 1.54$, which is greater than unity. Therefore, we have obtained, the DFE point $Q_0 = (1.28205 \times 10^9, 0, 0, 0)$ and the endemic equilibrium point $Q^* = (1.01476 \times 10^9, 265443, 319428, 1.61834 \times 10^8)$. For the value of $\beta = 6.4 \times 10^{-11}$, the DFE point $Q_0$ becomes unstable and $Q^*$ becomes stable, as in this case $\mathcal{R}_0 > 1$. The reproduction number $\mathcal{R}_0 > 1$ indicates that the spread of infection per infected individual has risen, which in turn, drastically increases the infected cases. Number of infected individuals rises at a steeper rate in the first $10$ days and then gently decreases to reach

Applications and Applied Mathematics: An International Journal (AAM), Vol. 15 [2020], Iss. 2, Art. 21

AAM: Intern. J., Vol. 15, Issue 2 (December 2020)                                    1063

**Figure 4.** Graphs justifying the local stability of the disease-free equilibrium point $Q_0 = (1.28205 \times 10^9, 0, 0, 0)$ for $\mathcal{R}_0 = 0.963531 < 1$

the value at $319428$. Also, the number of individuals actively infected with COVID-19 rises due to inadequate implementation of social distancing by exposed individuals and isolation of infectives. However, as infected individuals increase, the number of recovered individuals also rises at a faster rate than the number of infectives. Thus, neglecting the isolation of infectives, social distancing by exposed individuals, and major precautions by susceptibles and exposed individuals enforce $\mathcal{R}_0$ to be greater than unity and compel the endemic equilibrium point $Q^*$ to come into existence. Therefore, if $\mathcal{R}_0$ continues to increase at this rate, a large number of individuals in India become infected with COVID-19. Figure (3) indicates the prevalence of infection for $\mathcal{R}_0 > 1$.

In Figure 4, the results are portrayed for $\beta = 4.0 \times 10^{-11}$, which enforces the basic reproduction number $\mathcal{R}_0$ to reduce down below the unity at $0.963531$. Self quarantine of uninfected population and isolation of infectives, increase the effectiveness of the prevention measures ($\gamma_1$ and $\gamma_2$, respectively), which in turn reduce the force of infection for the disease transmission and thus, impose a huge impact on the threshold quality $\mathcal{R}_0$. If the transmission rate $\beta$ reduces to $4.0 \times 10^{-11}$, the number of infected individuals also decreases significantly. Number of individuals being exposed to COVID-19 disease rapidly starts diminishing and converges to zero. From the initial time, the number of exposed individuals starts falling down to approach zero, in a duration of around $500$ days. Due to rapid curtail in exposed individuals, the number of infected individuals also decreases effectively and approaches zero in approximately $500$ days. As the infected population rises initially, recovered individuals are rising continuously to reach its peak level and then start decreasing to approach zero, as infected individuals reach towards zero. After getting the treatment for COVID-19 disease, few recovered individuals will not get permanent immunity due to compromised immune systems and hence again become susceptible. Also, due to reduction in the amount

**Figure 5.** Graphs illustrating the influence of the transmission rate on population to justify the impact of prevention measures among individuals. The graphs are plotted by varying the transmission rate from $5.8 \times 10^{-11}$ to $6.4 \times 10^{-11}$ (a) Exposed individuals (b) Infected individuals (c) Number of recovered individuals

of spread of the COVID-19 disease, the number of infectives decreases which in turn, increases the number of susceptible to reach its maximum value for $\mathcal{R}_0 = 0.963531$. Therefore, to reduce $\mathcal{R}_0$ below one, precautionary measures such as infection prevention, social distancing and isolation of infectives must be essentially followed by all the classes of population. Figure 4, justifies the local stability of the disease-free equilibrium $Q_0 = (1.28205 \times 10^9, 0, 0, 0)$ for $\mathcal{R}_0 < 1$.

In Figure 5, we discuss the effects of transmission rate for four distinct values, that is, $\beta = 6.4 \times 10^{-11}$, $\beta = 6.2 \times 10^{-11}$, $\beta = 6.0 \times 10^{-11}$ and $\beta = 5.8 \times 10^{-11}$. The transmission rate measures the rate at which a susceptible individual acquires COVID-19 infection after coming in contact with an infected individual. As the transmission rate rises from $\beta = 5.8 \times 10^{-11}$ to $\beta = 6.4 \times 10^{-11}$, the threshold quantity $\mathcal{R}_0$ will be drastically changed and increases from $\mathcal{R}_0 = 1.397$ to $\mathcal{R}_0 = 1.54$. This indicates that the number of uninfected individuals following social distancing measures is getting lower and hence for $\mathcal{R}_0 = 1.54$, the number of infectives increases at a higher rate, in relation to $\mathcal{R}_0 = 1.397$ instead. As the number of infectives increases, the number of individuals being exposed to COVID-19 infection rises at a higher rate, due to inappropriate implementation of self quarantine and social distancing by the exposed population. For the transmission rate $\beta = 5.8 \times 10^{-11}$ the endemic equilibrium point is $(1.07454 \times 10^9, 206077, 247989, 1.2564 \times 10^8)$, whereas for $\beta = 6.4 \times 10^{-11}$, the endemic equilibrium point is computed as $(1.01476 \times 10^9, 265443, 319428, 1.61834 \times 10^8)$. This indicates that even with minimal increment in the rate of disease transmission, the number of individuals being exposed to the disease increases with a large proportion and hence infectives also increase with an enormous rate. However, since the total number of infected individuals has risen with a big fraction, this implies recovered individuals also increase eventually, whereas due to increment in $\beta$ susceptibles decrease as they become more prone to get infected with the disease. Therefore, an increment in the value of $\beta$ indicates that the prevention rules such as infection prevention, social

Applications and Applied Mathematics: An International Journal (AAM), Vol. 15 [2020], Iss. 2, Art. 21

AAM: Intern. J., Vol. 15, Issue 2 (December 2020) 1065

**Table 4.** The impact of variation in the effectiveness of prevention measures ($\gamma_2$) taken by infectives

| $\gamma_1$ | $\gamma_2$ | Susceptibles | Exposed | Infectives | Recovered |
|---|---|---|---|---|---|
| $8.5 \times 10^{-7}$ | $1 \times 10^{-7}$ | $9.32243 \times 10^8$ | 347390 | 418041 | $2.11795 \times 10^8$ |
| $8.5 \times 10^{-7}$ | $2 \times 10^{-7}$ | $9.51135 \times 10^8$ | 328628 | 395464 | $2.00356 \times 10^8$ |
| $8.5 \times 10^{-7}$ | $3 \times 10^{-7}$ | $9.67540 \times 10^8$ | 312336 | 375858 | $1.90424 \times 10^8$ |
| $8.5 \times 10^{-7}$ | $4 \times 10^{-7}$ | $9.81976 \times 10^8$ | 298001 | 358607 | $1.81683 \times 10^8$ |

distancing and isolation of infectives are not strictly followed and implemented in the community. The numerical simulations indicate that the threshold quantity $\mathcal{R}_0$, and the transmission rate $\beta$ must be rapidly reduced, otherwise the COVID-19 disease may become hazardous for the country.
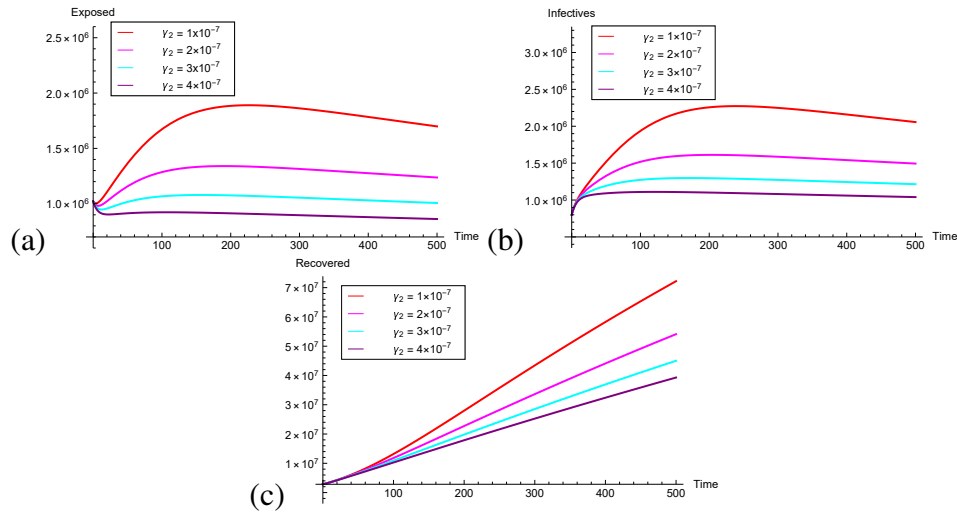
### 6.1. Impact of prevention measures

In this segment, we explore the effect of prevention measures followed by exposed individuals and infectives to reduce the infection prevalence. The inhibition effects measured in terms of prevention level including social distancing, isolation of infectives and taking proper precautions such as mask wearing, cleansing body and rigorous hand washing are depicted in Figure 6 and 7. In the model, $\gamma_1$ and $\gamma_2$ describe the effectiveness of the prevention measures taken by exposed and infected individuals, respectively.
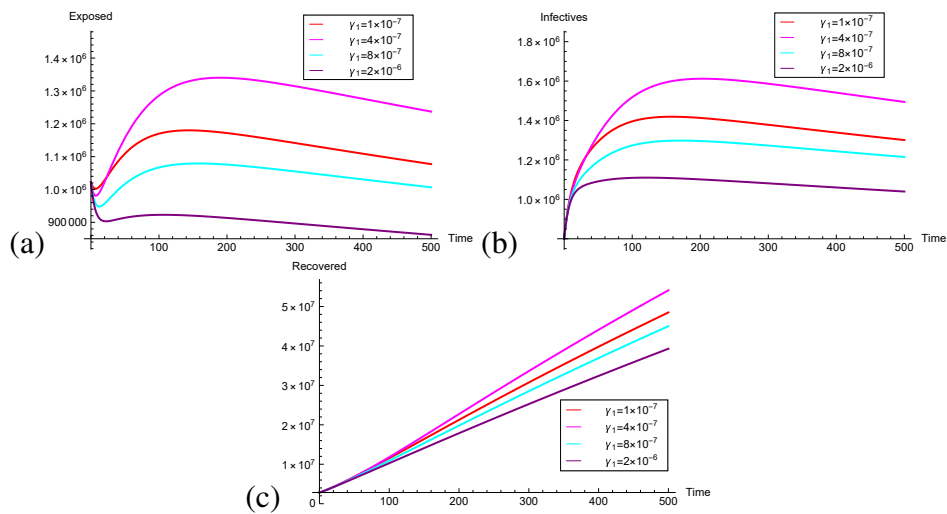
The impact of the level of preventions taken by the population of the infected class can be interpreted from Table (4). From the table, it can be observed that by keeping the value of $\gamma_1$ constant, number of susceptibles increases, together with increasing the value effectiveness of prevention measures followed by infectives, that is $\gamma_2$, from $1 \times 10^{-7}$ to $4 \times 10^{-7}$. Whereas, the number of exposed individuals, infectives and recovered individuals decrease with huge margins, due to a significant increment in the value of $\gamma_2$.

The results obtained in Figure 6, indicate the impact of effectiveness of prevention measures taken by infectives ($\gamma_2$), with a fixed value of $\gamma_1 = 8.5 \times 10^{-7}$, over susceptibles, exposed individuals, infectives and recovered individuals. In the figure, the graphs of different classes represent the comparison between the multiple curves of same class for four distinct values of the prevention rate: $\gamma_2 = 1 \times 10^{-7}$, $\gamma_2 = 2 \times 10^{-7}$, $\gamma_2 = 3 \times 10^{-7}$ and $\gamma_2 = 4 \times 10^{-7}$. From Figure 6(a), 6(b) and 6(c), it can be noticed that a small variation in prevention measures taken by the infected population positively change the level of disease in the community. Therefore, with the increment in $\gamma_2$, that is, improving isolation facilities for infectives, proper medicinal facilities to improve the immune system of infected individuals, more hindrance will be created for the virus to spread, and hence, the number of individuals suffering from the disease decreases.

In Figure 7, the results are depicted for a fixed value of $\gamma_2 = 6.8 \times 10^{-7}$ and taking four distinct values for $\gamma_1$, the effectiveness of prevention measures taken by the number of population being exposed to coronavirus, as $\gamma_1 = 1 \times 10^{-7}$, $\gamma_1 = 4 \times 10^{-7}$, $\gamma_1 = 8 \times 10^{-7}$ and $\gamma_1 = 2 \times 10^{-6}$. Increment in the value of $\gamma_1$, reduces the number of exposed individuals with marginal rate by tak-

**Figure 6.** Graphs indicating the impact of effectiveness of prevention measures$(\gamma_2)$, taken by infectives, induced by isolation and use of face masks on the population by varying $\gamma_2$ between $1 \times 10^{-7}$ and $4 \times 10^{-7}$ (a) Impact on individuals exposed to COVID-19 (b) Impact on COVID-19 infectives (c) Impact on recovered individuals



**Figure 7.** Graphs illustrating the effectiveness of prevention measures$(\gamma_1)$, taken by exposed individuals (induced quarantine, social distancing and use of face mask in public), ranges between $1 \times 10^{-7}$ and $2 \times 10^{-6}$ (a) Impact on exposed individuals (b) Impact on COVID-19 infectives (c) Impact on recovered individuals

**Table 5.** The impact of variation in the effectiveness of prevention measures$(\gamma_1)$, taken by exposed individuals

| $\gamma_1$ | $\gamma_2$ | Susceptibles | Exposed | Infectives | Recovered |
|---|---|---|---|---|---|
| $4 \times 10^{-7}$ | $6.8 \times 10^{-7}$ | $9.90076 \times 10^8$ | 289957 | 348927 | $1.76779 \times 10^8$ |
| $6 \times 10^{-7}$ | $6.8 \times 10^{-7}$ | $1.00203 \times 10^9$ | 278088 | 334644 | $1.69543 \times 10^8$ |
| $7 \times 10^{-7}$ | $6.8 \times 10^{-7}$ | $1.00738 \times 10^9$ | 272774 | 328249 | $1.66303 \times 10^8$ |

ing more precautions towards infection prevention and social distancing, which in turn influences the number of infectives as infected population diminishes initially with large proportion and then falls down with marginal rates as prevention measure $\gamma_1$ increases.

Applications and Applied Mathematics: An International Journal (AAM), Vol. 15 [2020], Iss. 2, Art. 21

AAM: Intern. J., Vol. 15, Issue 2 (December 2020)                                                                    1067

From Table (5), it can be analyzed that raising the value of $\gamma_1$ from $4 \times 10^{-7}$ to $7 \times 10^{-7}$, does not effectively increase the number of susceptibles, only slight improvement can be observed in the class of susceptibles. In a similar manner, a minor increment in the value of prevention level of exposed individuals does not provide a high impact in reducing the number of exposed individuals. This may happen, due to a less viral load on exposed individuals, and hence, lesser infectiousness of exposed individuals (signified by the parameter $\eta$) in comparison with actively infected individuals. In order to observe the significant impact of prevention measures taken by exposed individuals, a remarkable improvement in $\gamma_1$ is required by stringently obeying prevention measures such as, border screening, work from home, social distancing, self-quarantine and use of face masks in public.

The results depicted in Figure 6 and 7, imply that only with a huge increment in $\gamma_1$, the number of exposed individuals and infectives decrease effectively. However, only with a small increment in $\gamma_2$, the number of infectives and hence, exposed individuals decrease with a large proportion. Therefore, prevention measures for infectives are essentially required to implement in communities on a large scale.

From the numerical outcomes, we conclude that, to remove the spread of COVID-19 in India, influential headway treatment programmes, border screening, social distancing, self-quarantine awareness and isolation are prerequisites. Through this a significant reduction in COVID-19 disease can be achieved. The model, however, has few limitations such as limited accessibility of data as COVID-19 is a newly emerged disease. Thus, some parameters value have been assumed, instead of estimating from the given data. Even with this limitation, the given model provides the realistic information due to the incorporation of saturated incidence rate.

## 7.   Conclusion

Coronavirus outbreak has become a major concern for all the countries, especially for the countries with a large population. To pay adequate attention towards the transmission dynamics of COVID-19, we made assumptions to impose the current actions taken by the government. In this paper, a mathematical model has been proposed for COVID-19 disease by incorporating the saturated incidence rate for the transmission of coronavirus to understand the influence of government strategies such as isolation, infection prevention and social distancing on the spread of infection. The threshold quantity, which shapes the overall disease risk of the epidemic, known as the basic reproduction number $\mathcal{R}_0$, has been computed. By analysing the basic reproduction number, the location and the global asymptotic stability of the disease-free equilibrium point has been proved for $\mathcal{R}_0 < 1$. Whereas, the endemic equilibrium point comes into existence and has been proved to be locally asymptotically stable for $\mathcal{R}_0 > 1$, under certain restrictions on the parameters. To signify the importance of various parameters on the reproduction number, sensitivity analysis has been performed, which in turn justify the impact of various parameters in reducing the transmission of the disease.

Numerical simulations demonstrate the application of this paper on the transmission dynamics of

COVID-19 in India. From the numerical simulations, it has been observed that by reducing in the value of basic reproduction number, the spread of disease can be controlled. In sensitivity analysis, we came to realize that any change in the transmission rate directly affects the basic reproduction number. Therefore, the disease may come into a controlled situation, if the basic reproduction number is less than unity for which a remarkable reduction in the transmission rate of COVID-19 is required. According to the WHO report, it can be achieved by following social distancing, isolation and early treatment of infectives. The presence of saturated incidence rate in the force of infection for COVID$-19$ shows the impact of prevention measures taken by the exposed and infected individuals. To reduce the infection prevalence, reduction in the number of effective contacts between the infected individuals and the susceptibles is prerequisite, by strictly obeying quarantine of infectives and taking preventive measures by the uninfected population. It can also be observed that though the reproduction number does not depend explicitly on $\gamma_1$ and $\gamma_2$, the steady state value of infectives in the endemic state decreases as the level of prevention increases. To reduce the infection prevalence, strict obeying of control measures and policies such as home quarantine, border screening, wearing marks, social distancing and isolation of infectives, are essentially required. According to the scientific evidences, the early withdrawal of these strategies introduce undesirable results.

Thus, we conclude that to reduce the COVID-19 disease infection from the country, it is required to strictly follow the WHO guidelines such as social distancing activities, infection prevention and isolation of infectives, which in turn increase the prevention level and decrease the COVID-19 disease burden from the population.

# REFERENCES

Ahmad, S., Ullah, A., Al-Mdallal, Q. M., Khan, H., Shah, K. and Khan, A. (2020). Fractional order mathematical modeling of COVID-19 transmission, Chaos Soliton Fract., Vol. 139, 110256. https://doi.org/10.1016/j.chaos.2020.110256

Annas, S., Pratama, M. I., Rifandi, M., Sanusi, W. and Side, S. (2020). Stability analysis and numerical simulation of SEIR model for pandemic COVID-19 spread in Indonesia, Chaos Soliton Fract., Vol. 139, 110072. https://doi.org/10.1016/j.chaos.2020.110072

Awoke, T. D. and Semu, M. K. (2018). Optimal Control Strategy for TB-HIV/AIDS Co-Infection Model in the Presence of Behaviour Modification, Processes, Vol. 6, No. 5, 48. https://doi.org/10.3390/pr6050048

Applications and Applied Mathematics: An International Journal (AAM), Vol. 15 [2020], Iss. 2, Art. 21

AAM: Intern. J., Vol. 15, Issue 2 (December 2020)                                                                 1069

Carr, J. (1981) *Applications of center manifold theory*, Springer, New York.

Castillo-Chavez, C., Feng, Z. and Huang, W. (1999). On the computation of $\mathcal{R}_0$ and its role on global stability, in *Mathematical Approaches for Emerging and Reemerging Infectious Diseases: An Introduction*, IMA Vol. Math. Appl. 125, pp. 229–250, Springer, New York.

Castillo-Chavez, C. and Song, B. (2004). Dynamical models of tuberculosis and their applications, Math. Biosci. Eng., Vol. 1, No. 2, pp. 361–404. https://doi.org/10.3934/mbe.2004.1.361

Chen, T.M., Rui, J., Wang, Q.P., Zhao, Z.Y., Cui, J.A. and Yin, L. (2020). A mathematical model for simulating the phase-based transmissibility of a novel coronavirus, Infect. Dis. Poverty, Vol. 9, No. 1, 24. https://doi.org/10.1186/s40249-020-00640-3

Chitnis, N., Hyman, J.M. and Cushing, J.M. (2008). Determining important parameters in the spread of malaria through the sensitivity analysis of a mathematical model, Bull. Math. Biol., Vol. 70, pp. 1272âĂŞ1296. https://doi.org/10.1007/s11538-008-9299-0

CNN report (2020). https://edition.cnn.com/2020/06/09/health/asymptomatic-presymptomatic-coronavirus-spread-explained-wellness/index.html

Colbourn, T. (2020). COVID-19: extending or relaxing distancing control measures, Lancet Public Health, In press. https://doi.org/10.1016/S2468-2667(20)30072-4

Dongmei, X. and Ruan, S. (2007). Global analysis of an epidemic model with nonmonotone incidence rate, Math. biosci., Vol. 208, No. 2, pp. 419-429. https://doi.org/10.1016/j.mbs.2006.09.025

Driessche, P. van den and Watmough, J. (2002). Reproduction numbers and sub-threshold endemic equilibria for compartmental models of disease transmission, Math. Biosci., Vol. 180, pp. 29–48. https://doi.org/10.1016/S0025-5564(02)00108-6

Dubey, B., Patra, A., Srivastava, P. K. and Dubey, U. S. (2013). Modeling and analysis of an SEIR model with different types of nonlinear treatment rates, J. Biol. Systems, Vol. 21, No. 3, 1350023. https://doi.org/10.1142/S021833901350023X

ECDC (2020). Coronavirus disease 2019 (COVID-19) pandemic: increased transmission in the EU/EEA and the UK âĂŞ seventh update, 25 March 2020. Stockholm: ECDC.

Ferguson, N.M., Laydon, D., Nedjati-Gilani, G., Imai, N., Ainslie, K., Baguelin, M., Bhatia, S., Boonyasiri, A., Cucunubá, Z., Cuomo-Dannenburg, G., et al. (2020). Impact of Non-Pharmaceutical Interventions (NPIs) to reduce COVID-19 mortality and healthcare demand, Imperial College COVID-19 Response Team, London 16. https://doi.org/10.25561/77482

Hsu, S. B. and Hsieh, Y. H. (2005). Modeling intervention measures and severity-dependent public response during severe acute respiratory syndrome outbreak, SIAM J. Appl. Math., Vol. 66, No. 2, pp. 627-647. http://www.jstor.org/stable/4096131

India population live (2020) - Countrymeters: https://countrymeters.info/en/India

Jones, J. H. (2007) Notes on $\mathcal{R}_0$. https://web.stanford.edu/jhj1/teachingdocs/Jones-on-R0.pdf

Kucharski, A. J. et al. (2020). Early dynamics of transmission and control of COVID-19: a mathematical modelling study, Lancet Infect. Dis. https://doi.org/10.1016/S1473-3099(20)30144-4

Lin, Q. et al. (2020). A conceptual model for the coronavirus disease 2019 (COVID-19) outbreak in Wuhan, China with individual reaction and governmental action, Int. J. Infectious Diseases, Vol. 93, pp. 211-216. https://doi.org/10.1016/j.ijid.2020.02.058

Liu, J. (2019). Bifurcation analysis for a delayed SEIR epidemic model with saturated incidence and saturated treatment function, J. biol. dynam., Vol. 13, No. 1, pp. 461-480.

https://doi.org/10.1080/17513758.2019.1631965

Liu, X. and Yang, L. (2012). Stability analysis of an SEIQV epidemic model with saturated incidence rate, Nonlinear Anal. Real World Appl., Vol. 13, No. 6, pp. 2671-2679. https://doi.org/10.1016/j.nonrwa.2012.03.010

Mandal, M., Jana, S., Nandi, S. K., Khatua, A., Adak, S. and Kar, T. K. (2020). A model based study on the dynamics of COVID-19: Prediction and control, Chaos Soliton Fract., Vol. 136, 109889. https://doi.org/10.1016/j.chaos.2020.109889

Manyombe, M. L. M., Mbang, J., Nkamba, L. N. and Onana, D. F. N. (2020). Viral dynamics of delayed CTL-inclusive HIV-1 infection model with both virus-to-cell and cell-to-cell transmissions, Appl. Appl. Math., Vol. 15, No. 1, pp. 94–116.

Ministry of Health and Family Welfare (MoHFW). https://www.mohfw.gov.in/

Ndairou, F., Area, I., Nieto, J. J. and Torres, D.F.M. (2020). Mathematical modeling of COVID-19 transmission dynamics with a case study of Wuhan, Chaos Soliton Fract. https://doi.org/10.1016/j.chaos.2020.109846

Pang, L., Liu, S., Zhang, X., Tian, T. and Zhao, Z. (2020). Transmission dynamics and control strategies of COVID-19 in Wuhan, China, J. Biol. Syst., pp. 1-18. https://doi.org/10.1142/S0218339020500096

Perko, L. (1991). *Differential Equations and Dynamical Systems, Texts in Applied Mathematics*, 7, Springer-Verlag New York, Inc., New York.

Pradhan, S. P., Ferenc, H. and Turi, J. (2019). Dynamics in a respiratory control model with two delays, Appl. Appl. Math., Vol. 14, No. 2, pp. 863–874.

Prem, K. et al. (2020). The effect of control strategies to reduce social mixing on outcomes of the COVID-19 epidemic in Wuhan, China: a modelling study, Lancet Public Health. https://doi.org/10.1016/S2468-2667(20)30073-6

Quaranta, G., Formica, G., Machado, J. T., Lacarbonara, W. and Masri, S. F. (2020). Understanding COVID-19 nonlinear multi-scale dynamic spreading in Italy, Nonlinear Dyn., Vol. 288, pp. 1–37. https://doi.org/10.1007/s11071-020-05902-1

Shahidul, M. I., Irana, I. J., Kabir, K. M. A. and Kamrujjaman, M. (2020). COVID-19 epidemic compartments model and Bangladesh, Preprints. https://doi:10.20944/preprints202004.0193.v1

Statista (2020). https://www.statista.com/statistics/1041383/life-expectancy-india-all-time/

Strogatz, S. H. (2014). *Nonlinear Dynamics and Chaos: with Applications to Physics, Biology, Chemistry, and Engineering*, Westview press, Massachusetts.

Tanvi and Aggarwal, R. (2020a). Dynamics of HIV-TB co-infection with detection as optimal intervention strategy, Int. J. Nonlin. Mech., Vol. 120, 103388. https://doi.org/10.1016/j.ijnonlinmec.2019.103388

Tanvi and Aggarwal, R. (2020b). Stability analysis of a delayed HIV-TB co-infection model in resource limitation settings, Chaos Soliton Fract., Vol. 140, 110138. https://doi.org/10.1016/j.chaos.2020.110138

Tanvi, Aggarwal, R. and Kovacs, T. (2020). Assessing the effects of Holling Type-II treatment rate on HIV-TB co-infection, Acta Biotheor. https://doi.org/10.1007/s10441-020-09385-w

Wang, X., Tao, Y. and Song, X. (2009). Stability and Hopf bifurcation on a model for HIV infection of CD4+ T cells with delay, Chaos Soliton Fract., Vol. 42, No. 3, pp. 1838–1844.

Applications and Applied Mathematics: An International Journal (AAM), Vol. 15 [2020], Iss. 2, Art. 21

AAM: Intern. J., Vol. 15, Issue 2 (December 2020)                                                    1071

https://doi.org/10.1016/j.chaos.2009.03.089

Wilder-Smith, A. and Freedman, D.O. (2020). Isolation, quarantine, social distancing and community containment: pivotal role for old-style public health measures in the novel coronavirus (2019-nCoV) outbreak, J. Travel med. Vol. 27, No. 2. https://doi.org/10.1093/jtm/taaa020

World Health Organization (2020a). https://www.who.int/docs/default-source/coronaviruse/situation-reports/20200402-sitrep-73-covid-19.pdf

World Health Organization (2020b). https://www.who.int/health-topics/coronavirus#tab=tab$_1$

World Health Organization (2020c). https://www.who.int/emergencies/diseases/novel- coronavirus-2019

Worldometer (2020a). https://www.worldometers.info/coronavirus/ coronavirus-cases/

Worldometer (2020b): https://www.worldometers.info/coronavirus/country/india/

Yaghoubi, A. R. and Najafi, H. S. (2019). Non-Standard Finite Difference Schemes for Investigating Stability of a Mathematical Model of Virus Therapy for Cancer, Appl. Appl. Math., Vol. 14, No. 2, pp. 805–819.

Yang, C. and Wang, J. (2020). A Mathematical model for the novel coronavirus epidemic in Wuhan, China, AIMS Press. https://doi.org/10.3934/mbe.2020148

Zhang, X., Ma, R. and Wang, L. (2020). Predicting turning point, duration and attack rate of COVID-19 outbreaks in major Western countries, Chaos Soliton Fract., Data in Brief, 105830. https://doi.org/10.1016/j.chaos.2020.109829